



R_{out}/R_{sid} and Opacity at RHIC

Larry McLerran¹ and Sandra S. Padula^{1,2}

¹ *Nuclear Theory Group, Brookhaven National Laboratory, Upton, NY 11973, USA*

² *Instituto de Física Teórica, Universidade Estadual Paulista, São Paulo - SP, Brazil;*

Theoretical Physics, FERMILAB, Batavia, IL 60510, USA

Abstract

One of the most dramatic results from the first RHIC run are the STAR results for $\pi^\pm\pi^\pm$ interferometry. They showed that the ratio of the so-called R_{out} and R_{sid} radii seem to decrease below unity for increasing transverse momentum of the pair (K_T). This was subsequently confirmed by PHENIX which also extended the K_T range of the measurements. We consider here the effects of opacity of the nuclei on this ratio, and find that such a small value is consistent with surface emission from an opaque source.

I. INTRODUCTION

The striking result on $\pi^\pm\pi^\pm$ interferometry data obtained by STAR Collaboration [1] on the ratio R_{out}/R_{sid} is not yet understood. This is the ratio of the *outward* radius, measured in the correlation along the direction of the sum of the particles' momenta, divided by the *sideward* radius, reflecting the correlation perpendicular to the beam and perpendicular to the outward direction. This result was subsequently confirmed by PHENIX [2]. In an attempt to understand this result we consider in detail a generalization of the model used by Heiselberg and Vischer [3] to include effects of source opacity at CERN energies, later followed by Heinz and Tomášik [4].

The origin of the problem can be understood from the simplest model of HBT [5,6]. In this model we let particles be emitted from the entire volume of the system. In this case, the spatial size which is probed by R_{out} and R_{sid} is of the same order of magnitude, the radius of the system. However, R_{out} also has a spatial correlation built in on account of the time differences of different emissions [7]. R_{out} is the size scale measured along the particle's direction of motion. Particles emitted at much different times end up spatially separated from one another in this direction. We therefore expect that since the time separations are of the order of the size of the system (which for practical purposes seems to be a reasonable approximation for order of magnitude estimates at RHIC), then $R_{out}/R_{sid} > 1$. Most simple models incorporating the above physics give the ratio to be about $R_{out}/R_{sid} \sim 2$.

The assumption that the particles are emitted from the entire volume of the system is probably a bad one. Data on p_T distributions of particles in STAR [1] and PHENIX [2] suggest that the system is opaque to particles up to large transverse momenta. A more reasonable description might be blackbody surface emission.

To implement opacity, we consider a model where the matter is emitting from a surface at a fixed radius. The system is allowed to undergo 1 + 1 dimensional longitudinal expansion. The details of this model and its results are described in the fourth section. Many of the features of the model we propose are embodied in the hydrodynamic computations of Heinz and Kolb. [8] The essential difference lies in the treatment of surface emission.

An important ingredient of this model is decoupling, which we assume occurs at a well defined temperature. In the surface emission model we use, this requires that, at the end of the process, the decoupling to occur throughout the transverse volume of the system at a well defined time. It turns out that, although it is a relevant ingredient (i.e., it contributes to the *averaging* over different emission radii), this is not so important in our computations because the surface emission dominates.

In the second section, before turning to explicit model computations, we review the method of the Covariant Current Ensemble formalism for computing two particle HBT correlation functions. In this section, we try to be general enough to include the physics needed for our various computations.

In the third section, we consider a simpler version of the above model. We compute the various radii for the case of a cylinder emitting at a constant temperature T for a finite time Δt , without introducing any radial flow. We will consider both the case of an opaque source and a transparent one. In this oversimplified model, we show that in the opaque source limit, that $R_{out} \sim \sqrt{\Delta t^2 (K_T/E_K)^2 + (0.2R_T)^2}$ and $R_{sid} \sim R_T$. For the realistic case where $\Delta t \sim R_T$, $R_{out}/R_{sid} \sim \Delta t (K_T/E_K)/R_T$, and this ratio can be less than one. In the transparent limit $R_{out} = \sqrt{\Delta t^2 (K_T/E_K)^2 + R_T^2}$ and $R_{sid} \sim R_T$, this ratio is always larger than 1.

In the heavy ion experiments, the ratio R_{out}/R_{sid} is larger than 1 at AGS to SPS energies for $\pi^-\pi^-$ pairs [6,9]. For $\pi^+\pi^+$ it is also larger than 1 at AGS ($R_{out}/R_{sid} \approx 1.3$ - E859 Collab. [6,11]) but slightly smaller than 1 at SPS, according to NA44 data [6].

Although the value of R_{out}/R_{sid} is above one at the AGS, and it is relatively close to one at the SPS, [9]- [10], the data at RHIC gives an even smaller value. This suggests that at RHIC this ratio reflects the opacity of the emitting surface. The origin of the smaller value of R_{out}/R_{sid} for the opaque case is due to two effects. First, the system radiates from a smaller geometrical region than in the transparent case. Second, the emission itself is preferentially from the region of the cylinder closest to the radial vector made by \mathbf{R}_{out} , where this vector is a radial vector in the direction of the pair transverse momentum \mathbf{K}_T . This is because radiation from this region is normal to the surface, and there is a factor of $\cos \phi$ associated with the flux in the direction of \mathbf{R}_{out} , where ϕ is the angle between \mathbf{R}_{out} and a normal vector to the surface. Finally there is also the emission from the decoupling volume which occurs at a well defined time, which we shall see does not significantly contribute to the flux of particles, although it still contributes to the *averaging* over different emission radii.

The case of 1 + 1 dimensional longitudinal expansion is more complicated. In later sections, we shall use a simple model of the matter, where there is a real first order phase transition between a parton gas (gluons and massless quarks) and a pion gas. The energy is emitted from the partonic phase. This quark and gluon matter is assumed to be directly converted into a flux of pions with the same energy and a blackbody distribution at the temperature of emission. This energy conservation condition allows us to directly take a flux of gluons and quarks and convert it into a spectrum of pions. It of course will mess up details

of the fragmentation, and generates some increase in entropy, but for our purposes such a crude treatment is sufficient to demonstrate the physics of opacity in a semi-quantitative way. The emission of the hadron degrees of freedom is taken to be entirely pions. We will find that the dominant emission at RHIC energies comes from times after the beginning of the mixed phase, but there is a significant mixture of gluonic and quark radiation which must convert into pions.

The characteristic time scale for emission is of the order of the radius of the system before the radiation is significantly attenuated. This time scale is of the order of the size of the system for RHIC energies. Our model which incorporates this physics is described in detail in Sec. 4. In the fifth section, we describe some of the details of the computation of the HBT correlation function.

In the final section, we discuss the limitations of our approach. The severest is that if we try to predict the values of HBT radii as a function of K_T of the pair, we do not get the correct transverse momentum dependence. We do however get the correct K_T dependence for R_{out}/R_{sid} .

II. THE COVARIANT CURRENT ENSEMBLE INPUTS

To compute the emitted spectrum and the two particle distribution function, leading to the interferometry relations in which we are interested, we consider the Covariant Current Ensemble formalism, [14], [15]. In this formalism, the two particle correlation function can be written as

$$C(k_1, k_2) = \frac{P_2(k_1, k_2)}{P_1(k_1)P_1(k_2)} = 1 + \frac{|G(k_1, k_2)|^2}{G(k_1, k_1)G(k_2, k_2)} \quad (1)$$

where $P_1(k_i)$ and $P_2(k_1, k_2)$ are, respectively, the single particle distribution and the probability for simultaneous observation of two particles with momenta k_1 and k_2 . The average momentum of the pair is defined as $\mathbf{K} = (\mathbf{k}_1 + \mathbf{k}_2)/2$, and the relative momentum, as $\mathbf{q} = \mathbf{k}_1 - \mathbf{k}_2$.

The complex amplitude, $G(k_1, k_2)$, is written as

$$G(k_1, k_2) = \int d^4p \int d^4x e^{iq^\mu x_\mu} D(x, p) j_0^*\left(\frac{k_1 \cdot p}{m}\right) j_0\left(\frac{k_2 \cdot p}{m}\right) , \quad (2)$$

and the single-inclusive distribution, $G(k_i, k_i)$, is written as

$$G(k_i, k_i) = \int d^4p \tilde{D}(0, p) |j_0\left(\frac{k_i \cdot p}{m}\right)|^2 = \frac{d^3\mathcal{N}}{d^2k_i dy} = E_i \frac{d^3\mathcal{N}}{d^3k_i} = P_1(k_i) . \quad (3)$$

We see that

$$\tilde{D}(q, p) = \int d^4x e^{iq^\mu x_\mu} D(x, p) , \quad (4)$$

where $D(x, p)$ is the normalized phase-space distribution at the instant of the emission.

One should note that there is some arbitrariness in how we decompose into $D(x, p)$ and the densities j_0 . We shall follow the original proposition in [14], [15], and choose to

include the thermal aspects of the collision in j_0 , and the geometrical plus collective effects in $D(x, p)$. In any case both will be defined for the problems at hand.

There are several different possibilities for $D(x, p)$:

The first is radiation from a transparent cylinder which is not expanding in the transverse directions and has no longitudinal expansion.

$$D(x, p) = g_p \kappa \exp(-t^2/2\Delta t^2) \delta(E_p - p^0) \delta^2(\mathbf{p}_T) \delta(p_z) \quad . \quad (5)$$

In this expression p is to be interpreted as the momentum of a particle at rest in the matter from which it is emitted, and reflects the collective motion of the system. For matter at rest, $\mathbf{p} = 0$. The factor g_p counts the number of degrees of freedom of particle being emitted. The factor of $e^{-t^2/2\Delta t^2}$ is a Gaussian parameterization of the source emission rate, so that the characteristic emission time is Δt . (The blackbody rate emerges naturally in this picture, and κ is a factor which modifies beyond the blackbody rate).

The second case is emission from the surface of a cylinder without longitudinal expansion. Here we must account for the fact that the particle is emitted with a flux factor which depends upon the angle ϕ between the normal vector to the surface and the direction of the pair transverse momentum \vec{K}_T . There is also a factor of $\delta(r_T - R_T)$ which requires that particles are emitted from the surface and a factor of $\Theta(\cos \phi)$ which requires they come from the side of the surface from which they are emitted.

$$D(x, p) = g_p \kappa \exp(-t^2/2\Delta t^2) \delta(r_T - R_T) \delta(E_p - p^0) \delta^2(\mathbf{p}_T) \delta(p_z) \cos \phi \Theta(\cos \phi) \quad . \quad (6)$$

Finally, there is the case of emission from the surface of a cylinder with longitudinal expansion

$$D(x, p) = g_p \kappa \delta(r_T - R_T) \delta(E_p - p^0) \delta^2(\mathbf{p}_T) \delta(y - \eta) \cos \phi \Theta(\cos \phi) \quad , \quad (7)$$

The factor of $\delta(y - \eta)$ is the correlation between the velocity and coordinate of the emitting surface built into the Bjorken model [12]. The factor of κ controls the rate of emission from the surface as a function of time. We will fix this by requiring the system to be either a Quark Gluon Plasma, a hadron gas or a mixture, with blackbody radiation and the mixture determined by thermodynamics.

The currents correspond to thermal distributions and are written as

$$J_0\left(\frac{k_i \cdot p}{m}\right) = \sqrt{u^\mu k_{i\mu}} \exp\left\{-\frac{u^\mu k_{i\mu}}{2T(\tau)}\right\} \quad . \quad (8)$$

Here $u^\mu = p^\mu/m$ is the four vector flow velocity which is the four velocity of the emitting surface. In the case where the currents are connected to the models illustrated by Eq. (5)-(6) above, $u^\mu = (1, \mathbf{0})$, i.e., associated to the absence of expansion along the longitudinal and transverse directions in those cases. We indicate by $T(\tau)$ the dependence of the temperature in the proper time, τ , prior to the beginning of the mixed phase, as given by Eq.(17), in Section IV.

In the ideal Bjorken picture with no transverse flow, the 4-velocity u^μ and the momentum of the emitted particle, k^μ , can be written as

$$u^\mu = (\cosh \eta, 0, 0, \sinh \eta) ; k^\mu = (m_T \cosh y, \mathbf{k}_T, m_T \sinh y) \quad . \quad (9)$$

III. A VERY SIMPLE MODEL FOR R_{out}/R_{sid}

We first work out the simplest model for emission so that we can get some conceptual understanding of the physics involved in the various cases. We shall consider a system without radial flow. The approximations will be fixed in the next section when we consider a more realistic model which we compare with data.

First consider emission from a transparent cylinder. A little algebra gives

$$C_{out} = 1 + \exp\left[-\frac{K_T^2 q_{out}^2 \Delta t^2}{(K^2 + m^2)}\right] [2J_1(q_{out}R_T)/(q_{out}R_T)]^2 \quad (10)$$

and

$$C_{sid} = 1 + [2J_1(q_{sid}R_T)/(q_{sid}R_T)]^2, \quad (11)$$

where $J_1(x)$ is the Bessel function of the first kind and order one.

In this equation, it is absolutely clear that $R_{out} > R_{sid}$, and that if $\Delta t \sim R$, then $R_{out} \sim 2R_{sid}$

Now let us consider the result for surface emission. In this case, a little algebra yields

$$C_{out} = 1 + \exp\left[-\frac{K_T^2 q_{out}^2 \Delta t^2}{(K^2 + m^2)}\right] |I(q_{out}R_T)|^2 \quad (12)$$

where

$$I(x) = \frac{1}{2} \int_0^\pi d\phi \sin(\phi) \exp[ix \sin(\phi)] \quad (13)$$

On the other hand,

$$C_{sid} = 1 + \left| \frac{\sin(q_{sid}R_T)}{(q_{sid}R_T)} \right|^2 \quad (14)$$

In Fig. 1, we plot C_{sid} and, for stressing the geometrical differences only, we ignored the time contribution to C_{out} , by fixing $\Delta t = 0$ in the plots. Fitting the curves by Gaussian distributions, we find that, in the opaque case, $R_{sid}^{eff} \approx R_T \times 0.53$ and $R_{out}^{eff} = R_T \times 0.22$. In the transparent case, the fit results in an effective radius of $R_{out}^{eff} \approx 0.61R_T$.

The basic result we get from this analysis is that for the opaque cylinder, unlike the transparent one, we can easily have $R_{out} < R_{sid}$. In fact for $R_{out} \sim \Delta t(K_T/E_K)$ (since the R_T contribution is very small), the ratio of $R_{out}/R_{sid} \sim \Delta t(K_T/E_K)/R_T$ unlike the transparent cylinder case where $R_{out}/R_{sid} \sim \sqrt{\Delta t^2(K_T/E_K)^2 + R_T^2}/R_T$.

IV. A SIMPLE MODEL FOR R_{out}/R_{sid}

In this model, we incorporate longitudinal expansion. Here the system cools as it expands, so we need to have the rate of emission vary as a function of time.

We need to have dynamical description of the microphysics to be able to do this. Our more or less conventional model is a Quark-Gluon Plasma (QGP) phase at some temperature

above the critical temperature, $T_0 > T_c$. We choose this critical temperature $T_c = 175$ MeV to be consistent with lattice Monte-Carlo data. The system goes into a mixed phase of QGP and hadron gas at the critical temperature, and we take this hadronic gas to be composed of an ideal gas of pions. Below T_c , it is only an ideal gas of pions. While in the low temperature pionic phase, the system cools until it reaches a decoupling temperature, T_f . We choose $T_f = 150$ MeV to be consistent with the typical energy per particle observed in the RHIC experiments, and to fit the observed p_T distributions of pions. However, these values chosen for T_c and T_f are not crucial for qualitatively reproducing the results we discuss here, since these results are only weakly sensitive to these particular values.

The system produced in a heavy ion collision will expand and the temperature will gradually decrease. The initial expansion is in the Quark-Gluon Plasma phase, and the system expands longitudinally. After this initial stage, lasting $(\tau_c - \tau_0)$, the transition temperature, T_c , is reached and the evolution continues in the mixed phase, during which the temperature remains constant with time. The mixed phase continues for a longer period, ending after an elapsed interval $(\tau_h - \tau_c)$. Then, the system converted into a gas of pions, further expands until the decoupling temperature, T_f , is reached. At this point, the system is quite dilute, and much of the particles have been evaporated from its surface. Thus, we consider that, once T_f is reached, the system decouples in an instantaneous volumetric emission.

The Bjorken hydrodynamical model [12] should be able to describe the system during its evolution from formation until the time it breaks up. We will supplement this with radiation from the surface of the matter. We will take the radius at which this radiation takes place to be a constant and equal to the radius of the nuclei. We only consider impact parameter zero collisions. In the last stage of the system evolution we consider a volumetric emission at freeze-out but, as in the surface emission, no transverse flow was introduced in the computation. This could be one of the main reasons for obtaining a much weaker K_T decrease of the transverse radii, as compared to RHIC data [1,2].

Another ingredient in our model is the hypothesis that the system will emit from its external surface similarly to a blackbody, starting shortly after being formed, at $\tau = \tau_0$. In this way, quark and gluon degrees of freedom have to be considered in the QGP and mixed phases. The hadronic degrees of freedom should, in principle, include a complete set of resonances later decaying into pions. However, in this initial description, and for the sake of simplicity, we will consider a hadronic gas constituted of only pions. No complex mechanism for the QGP hadronization will be considered in detail at this point, although hadronization must take place. In other word, in first approximation, we will consider the evaporation of “gluons” and “quarks” (as hadronized pions) from the external surface of the system in the same way as emission of pions, except for the number of degrees of freedom.

We can estimate the emitted energy as well as the total entropy associated to each stage. In the initial phase, lasting from τ_0 to τ_c , we can estimate the emitted energy as a function of time considering the emission by an expanding cylinder of transverse radius R_T and length h , in a certain time interval between τ and $\tau + d\tau$ by

$$dE_{in} = -\kappa\sigma T^4 2\pi R_T h d\tau - \frac{4}{3} \sigma T^4 \pi R_T^2 dh , \quad (15)$$

where the first term comes from the blackbody type of energy radiated from the surface of the cylinder, and the second term results from the mechanical work due to its expansion.

The κ factor was introduced to take into account that the system has some opacity to surface emission. The constant σ is proportional to the number of degrees of freedom in the system.

By integrating Eq. (15) we get for the energy density (i.e., $\epsilon = E/V$)

$$\epsilon_{in} = \epsilon_0 \left(\frac{\tau_0}{\tau}\right)^{\frac{4}{3}} e^{-\frac{2\kappa}{R_T}(\tau-\tau_0)} . \quad (16)$$

From the above expression we see that we obtain an extra multiplicative factor, $e^{-\frac{2\kappa}{R_T}(\tau-\tau_0)}$, in addition to that coming from the Bjorken picture. Remembering that, in the Bjorken picture, the relation between the energy density, ϵ , and the proper-time, τ , is given by $\epsilon/\epsilon_0 = (\tau_0/\tau)^{4/3}$, and that $\epsilon = \sigma T^4$ for a blackbody-type radiation, then the variation of the temperature in the initial stage, i.e., prior to the beginning of the phase transition, follows immediately as

$$T(\tau) = T_0 \left(\frac{\tau_0}{\tau}\right)^{\frac{1}{3}} e^{-\frac{\kappa}{2R_T}(\tau-\tau_0)} . \quad (17)$$

In order to fix the initial conditions of the evaporating and expanding fireball, we follow the evolution of the entropy, using the observed final particle multiplicity density dN/dy and its relation to the final entropy density dS/dy as a constraint. We decompose the total entropy S_{tot} into its contributions S_{in} from the fireball interior and from the emitted particles S_{emit} , all of which are functions of the proper-time. During the first stage, from τ_0 to the beginning of the mixed phase at time τ_c we can write

$$s_{in} = \frac{S_{in}}{V} = \frac{1}{T}(\epsilon + p)_{in} = s_0 \left(\frac{\tau_0}{\tau}\right) e^{-\frac{3\kappa}{2R_T}(\tau-\tau_0)} \rightarrow S_{in} = S_0 e^{-\frac{3\kappa}{2R_T}(\tau-\tau_0)} , \quad (18)$$

where $s_0 = \frac{4}{3}(\sigma\epsilon_0^3)^{1/4}$ is the initial entropy density. In the second step of Eq. (18) we used that, for the Bjorken type of longitudinal expansion, the volume $V(\tau)$ increases linearly with time.

On the other hand, the entropy associated with the emission can be estimated by

$$\frac{dS_{emit}}{V} = \frac{2\kappa}{R_T} s_{in} d\tau = \frac{2\kappa}{R_T} s_0 \left(\frac{\tau_0}{\tau}\right) e^{-\frac{3\kappa}{2R_T}(\tau-\tau_0)} d\tau \rightarrow S_{emit} = \frac{4}{3} S_0 [1 - e^{-\frac{3\kappa}{2R_T}(\tau-\tau_0)}] . \quad (19)$$

The factor of $2/R_T$ in the above expression comes from the ratio of the surface area of emission of the longitudinally expanding Bjorken system, $2\pi R d\tau$, divided by the Bjorken volume, $\pi R^2 d\tau$. This results in the total entropy of the initial stage as being

$$S_{tot} = \frac{4}{3} S_0 - \frac{1}{3} S_0 e^{-\frac{3\kappa}{2R_T}(\tau-\tau_0)} , \quad (20)$$

so that, at $\tau = \tau_0 \rightarrow S_{tot} = S_0$. Note that this result requires that there be entropy produced during the emission from the surface with the added input that the temperature changes as a function of time. In the mixed phase there will be no such effect, since there the emitted quanta are simply the number of the quanta in the system, and no entropy increase in particle number is generated. Note that the entropy for a massless gas is directly proportional to particle number. The situation is simply different when one has an expanding system with a variable temperature.

During the phase transition, the energy and entropy can be estimated similarly, leading to

$$\tilde{E}_{emit} = \tilde{E}_c(1 - e^{-\frac{2\kappa}{R_T}(\tau-\tau_c)}) ; \tilde{S}_{in} = \tilde{S}_c e^{-\frac{2\kappa}{R_T}(\tau-\tau_c)} ; \tilde{S}_{emit} = \tilde{S}_c(1 - e^{-\frac{2\kappa}{R_T}(\tau-\tau_c)}) . \quad (21)$$

These results follow simply from Eq. (15) when the second term on the right hand side is set to zero. During the mixed phase no work is done in expansion because the temperature does not change and the expansion conserves entropy. Therefore only the first term on the right hand side of Eq. (15) contributes, and it is easy to integrate, since it is $2\kappa E d\tau/R$.

From the above relations we can see that, during the phase transition, the total entropy, $\tilde{S}_{tot} = \tilde{S}_{in} + \tilde{S}_{emit} = \tilde{S}_c$ is conserved. During this extended period, the temperature remains constant with time ($T = T_c$), so that the previous relation in Eq. (17) no longer holds. Note that there is a difference in the exponential behavior in the mixed phase relative to that in the QGP phase. This is a consequence of the fact that the temperature is time dependent in the QGP phase, but time independent in the mixed phase, so that in the first case the rate of emission from the surface is different.

During the phase transition the system is in a mixed phase of Quark-Gluon Plasma and hadronic gas. If the fraction of the fluid in the QGP phase is f , then in the hadronic (pion) phase it would be $(1 - f)$. On the other hand, from Eq. (21), we see that the portion of the entropy density still in the system is given by $\tilde{s}_{in} = \tilde{s}_c(\frac{\tau_c}{\tau}) \exp[-\frac{2\kappa}{R_T}(\tau - \tau_c)]$. Consequently, $\tilde{s}_{in} = f \tilde{s}_{QGP} + (1 - f) \tilde{s}_h$, where $\tilde{s}_{in}(\tau_c) = \tilde{s}_c$ and $\tilde{s}(\tau_h) = \tilde{s}_c(\frac{\tau_c}{\tau_h}) \exp[-\frac{2\kappa}{R_T}(\tau_h - \tau_c)]$. If we substitute these expressions into that for \tilde{s}_{in} , we then get

$$f = \left(\frac{\tau_h e^{-\frac{2\kappa}{R_T}(\tau-\tau_c)} - \tau e^{-\frac{2\kappa}{R_T}(\tau_h-\tau_c)}}{\tau_h - \tau_c e^{-\frac{2\kappa}{R_T}(\tau_h-\tau_c)}} \right) \frac{\tau_c}{\tau} \quad ; \quad (1 - f) = \left(\frac{\tau - \tau_c e^{-\frac{2\kappa}{R_T}(\tau-\tau_c)}}{\tau_h - \tau_c e^{-\frac{2\kappa}{R_T}(\tau_h-\tau_c)}} \right) \frac{\tau_h}{\tau} . \quad (22)$$

Finally, we need to estimate the initial values T_0 and τ_0 , as well as the proper time, τ_c , corresponding to the on-set of the phase transition. We estimate τ_0 by means of the Uncertainty Principle, i.e., $\langle E_0 \rangle \tau_0 \approx \hbar$, and by

$$\langle E_0 \rangle = \frac{\int dp p^3 e^{-p/T_0}}{\int dp p^2 e^{-p/T_0}} = 3T_0 , \quad (23)$$

from which we easily determine the initial time as

$$\tau_0 \sim \frac{\hbar}{3T_0} = \frac{0.197}{3(T_0/\text{GeV})} \text{fm}/c . \quad (24)$$

On the other hand, the constraint on T_0 and τ_0 has to come from the experiment. At RHIC, the average produced pion multiplicity per unit of rapidity is $\mathcal{N} \sim 1000$, which should be proportional to the initial entropy, S_0 , i.e.,

$$S_0 = \Gamma \mathcal{N} = \left[(g_g + g_q) \times \left(\frac{4}{3} \right) \frac{\pi^2}{30} T_0^3 \right] \pi R_T^2 \tau_0 . \quad (25)$$

In the above expression, we have related the initial entropy, $S_0 = s_0 V_0$ to the initial entropy density and the initial volume of the system, $V_0 = \pi R_T^2 \tau_0$, this last one estimated in the Bjorken fashion. The degeneracy factors, g , are given by the gluon degrees of freedom,

$g_g = 2(\text{spin}) \times 8(\text{color})$, and the quark/anti-quark degrees of freedom, $g_q = \frac{7}{8}[2(\text{spin}) \times 2(q + \bar{q}) \times 3(\text{color}) \times N_f(\text{flavor})]$, which add up to $g_{qgp} = g_g + g_q$. In the case of pions, the degeneracy factor is $g_\pi = 3$.

From Eq.(24) and (25) we can determine T_0 as

$$T_0 = \sqrt{\mathcal{N}\Gamma} \left[(g_g + g_q) \times \frac{4\pi^3}{270} \frac{R_T^2}{(0.197)^2} \right]^{-1/2} \text{ GeV} . \quad (26)$$

As an example, if we take $\Gamma = 3.6$, as estimated by the entropy per particle (S_π/N_π) of a pion gas at freeze-out, then $T_0 \sim 411$ MeV and $\tau_0 \sim 0.160$ fm.

For estimating the instant corresponding to the beginning of the mixed phase, τ_c , we consider Eq.(17) at $\tau = \tau_c$, resulting in

$$\tau_c e^{\frac{3\kappa}{2R_T}\tau_c} = \left(\frac{T_0}{T_c} \right)^3 \tau_0 e^{\frac{3\kappa}{2R_T}\tau_0} , \quad (27)$$

which can be numerically estimated for fixed values of κ and T_c (for this, we will consider $T_c = 175$ MeV).

In order to estimate the instant corresponding to the end of the mixed phase, τ_h , we need to know \tilde{s}_c and \tilde{s}_h . For the first one, we consider a system of gluons and (massless) quarks forming an ideal gas, resulting in $\tilde{s}_c = (g_g + g_q) \frac{2\pi^2}{45} T_c^3$. For estimating τ_h , we consider the pions as massless particles, while in the system, leading to $\tilde{s}_h = g_\pi \frac{2\pi^2}{45} T_c^3$. Then, equating the expression for \tilde{s}_{in} at $\tau = \tau_h$, we obtain

$$\tau_h e^{\frac{2\kappa}{R_T}\tau_h} = \left(\frac{g_g + g_q}{g_\pi} \right) \tau_c e^{\frac{2\kappa}{R_T}\tau_c} , \quad (28)$$

which can be estimated numerically for a fixed value of κ , since τ_c was already determined by Eq. (27).

We assume that, at the end of the phase transition, corresponding to $\tau = \tau_h$, the system is an ideal gas of pions (no resonances are considered in this initial estimate), which continues to expand and cool down, until the temperature drops to $T_c = 150$ MeV, corresponding to an instant $\tau = \tau_f$. At this point, whatever is remnant of the system breaks up. The portion of the pions still in the system at that time we call \mathcal{V} , i.e., the fraction of the system that is emitted from the entire volume at the time τ_f . This decoupling instant can be estimated by an expression similar to Eq.(17)), with T_0 replaced by T_c , and τ_0 by τ_c , resulting in

$$\tau_f e^{\frac{3\kappa}{2R_T}\tau_f} = \left(\frac{T_c}{T_f} \right)^3 \tau_h e^{\frac{3\kappa}{2R_T}\tau_h} , \quad (29)$$

which can be numerically estimated for fixed values of κ , T_c , and T_f , and corresponding τ_h .

We illustrate in Table 1 below these variables for two different assumptions on the emissivity, κ . The values of the temperatures considered were $T_0 \sim 411$ MeV (obtained from Eq. (26)), $T_c = 175$ MeV and $T_f = 150$ MeV. We also include the corresponding estimates of the fraction of particles emitted from the surface, \mathcal{S} , in the interval $\tau_0 \leq \tau \leq \tau_f$, as well as the fraction from the volumetric emission, \mathcal{V} , at $\tau = \tau_f$.

To estimate the fraction of the particles emitted from the surface, \mathcal{S} , and from the volume, \mathcal{V} , we proceed as follows, estimating the contribution from each stage of the system evolution. For that, we estimate the emitted entropy in each stage, similarly to the procedure described in Eq.(18)-(21).

The fraction of the input particles, \mathcal{N} , emitted in the first period, $\tau_0 \leq \tau \leq \tau_c$, is given by

$$\frac{\mathcal{N}_1}{\mathcal{N}} = \frac{4}{3} (1 - e^{-\frac{3\kappa}{2R_T}(\tau_c - \tau_0)}) . \quad (30)$$

Similarly, the fraction $\mathcal{N}_2/\mathcal{N}$ emitted during the phase transition, $\tau_c \leq \tau \leq \tau_h$, can be written as

$$\frac{\mathcal{N}_2}{\mathcal{N}} = e^{-\frac{3\kappa}{2R_T}(\tau_c - \tau_0)} (1 - e^{-\frac{2\kappa}{R_T}(\tau_h - \tau_c)}) . \quad (31)$$

The fraction emitted during the pure pion phase, $\tau_h \leq \tau \leq \tau_f$, up to reaching T_f , can be estimated by

$$\frac{\mathcal{N}_3}{\mathcal{N}} = \frac{4}{3} e^{-\frac{3\kappa}{2R_T}(\tau_c - \tau_0)} e^{-\frac{2\kappa}{R_T}(\tau_h - \tau_c)} (1 - e^{-\frac{3\kappa}{2R_T}(\tau_f - \tau_h)}) . \quad (32)$$

Then, the fraction of the particles emitted from the surface up to $\tau = \tau_f$ is

$$\frac{\mathcal{S}}{\mathcal{N}} = \frac{1}{\mathcal{N}} (\mathcal{N}_1 + \mathcal{N}_2 + \mathcal{N}_3) . \quad (33)$$

Finally, the remnant fraction at $\tau = \tau_f$, emitted from the entire volume, is given by

$$\frac{\mathcal{V}}{\mathcal{N}} = \frac{\mathcal{N}_4}{\mathcal{N}} = e^{-\frac{3\kappa}{2R_T}(\tau_c - \tau_0)} e^{-\frac{2\kappa}{R_T}(\tau_h - \tau_c)} e^{-\frac{3\kappa}{2R_T}(\tau_f - \tau_h)} . \quad (34)$$

As a result, the ratio of the total number of emitted particles, \mathcal{N}_{tot} , with respect to the input number, \mathcal{N} , is given by

$$\frac{\mathcal{N}_{\text{tot}}}{\mathcal{N}} = \frac{1}{\mathcal{N}} (\mathcal{N}_1 + \mathcal{N}_2 + \mathcal{N}_3 + \mathcal{N}_4) . \quad (35)$$

TABLE 1: Values of the proper-time parameters τ_0 , τ_c , τ_h , τ_f , as well as of the surface, \mathcal{S} (for $\tau_0 \leq \tau \leq \tau_f$), and the volume, \mathcal{V} (at τ_f), emitted fluxes, for two values of the emissivity, κ .

κ	τ_0 (fm/c)	τ_c (fm/c)	τ_h (fm/c)	τ_f (fm/c)	\mathcal{S}/\mathcal{N} ($\tau_0 \leq \tau \leq \tau_f$)	\mathcal{V}/\mathcal{N} (at τ_f)
1	0.160	1.54	5.73	6.97	0.932	0.172
0.5	0.160	1.75	8.37	10.5	0.816	0.260

As we can see from the fractions in Table 1 above, in our model there is a small increment ($\sim 7.6 - 10\%$) in the total number of particles with respect to the initial one. We show in Fig. 2 the evolution of the emitted flux with proper time, by plotting the fractions normalized to the total number of produced pions, as a function of τ . The two different cases correspond to different surface emissivities. The curves end at the decoupling temperature. In the case of the greatest rate of surface emission, about 84% of the total radiation comes from the surface and the rest from the decoupling volume. It is about 76% for the other case we show for illustration. In the first case, the system decouples at a time of about 7 fm/c and in the second case at about 10.5 fm/c. We assume a decoupling temperature of 150 MeV. We should note that the decoupling proper-times within our model are significantly shorter than those in hydrodynamics. This is mainly due to the fact that we allowed a higher surface emissivity than those kind of models, which may be the key to explain the proper-times observed at RHIC, which are smaller than expected from hydro predictions.

V. SINGLE- AND TWO-PARTICLE PROBABILITY DISTRIBUTIONS

We define the average momentum of the pair as $K = \frac{1}{2}(k_1 + k_2)$ and the relative momentum as $q = (k_1 - k_2)$. They satisfy $q^\mu K_\mu = 0$, and, consequently, the temporal component of q^μ can be written as $q^0 = \frac{\mathbf{q}\cdot\mathbf{K}}{K^0}$. In the limit that is interesting for interferometry, we can consider $|\mathbf{q}| \ll |\mathbf{K}|$, which implies that $K^0 \approx \sqrt{|\mathbf{K}|^2 + m^2} = E_K$.

In both expressions for $C(k_1, k_2)$ and $C(k_i, k_i)$, we see that, due to the form of the phase-space distribution in Eq.(7), integration over the variables involving delta functions are straightforward. We should remember that, due to the factor $\Theta(\cos \phi)$ in Eq.(7), the integration over $d\phi$ runs in the interval $[-\pi/2, \pi/2]$, while the limits on the proper time integration would be $[\tau_0, \tau_f]$. However, as the system has different composition in each phase, we should split this time integration to be $[\tau_0, \tau_c]$, $[\tau_c, \tau_h]$, and then $[\tau_h, \tau_f]$. The rapidity integration should run, in the Bjorken picture, from $(-\infty, +\infty)$.

We recall that f and $(1 - f)$ are, respectively, the fractions of the system in the QGP phase and in the hadronic phase, according to the expression given in Eq.(22). Then, by taking into account the above observations, the expression for the complex amplitude, after some algebraic manipulation, can finally be written as

$$\begin{aligned}
G(k_1, k_2) &\propto \kappa R_T \int_{-\frac{\pi}{2}}^{\frac{\pi}{2}} d\phi \cos \phi \int_{-\infty}^{+\infty} dy [E_K \cosh y - K_L \sinh y] \\
&e^{-iq_T R_T \cos(\alpha - \phi)} \{g_{qgp} \int_{\tau_0}^{\tau_c} \tau d\tau e^{i\tau[\frac{K_T}{E_K} q_T \cos \alpha \cosh y + q_L (\frac{K_L}{E_K} \cosh y - \sinh y)]} \\
&\exp \left[-\frac{1}{T_0} (E_K \cosh y - K_L \sinh y) \left(\frac{\tau}{\tau_0} \right)^{1/3} e^{\kappa(\tau - \tau_0)/(2R_T)} \right] + \\
&g_{qgp} \int_{\tau_c}^{\tau_h} \tau d\tau (f) e^{i\tau[\frac{K_T}{E_K} q_T \cos \alpha \cosh y + q_L (\frac{K_L}{E_K} \cosh y - \sinh y)]} e^{-\frac{1}{T_c} (E_K \cosh y - K_L \sinh y)} + \\
&g_\pi \int_{\tau_c}^{\tau_h} \tau d\tau (1 - f) e^{i\tau[\frac{K_T}{E_K} q_T \cos \alpha \cosh y + q_L (\frac{K_L}{E_K} \cosh y - \sinh y)]} e^{-\frac{1}{T_c} (E_K \cosh y - K_L \sinh y)} +
\end{aligned}$$

$$\begin{aligned}
& g_\pi \int_{\tau_h}^{\tau_f} \tau d\tau e^{i\tau[\frac{K_T}{E_K} q_T \cos \alpha \cosh y + q_L (\frac{K_L}{E_K} \cosh y - \sinh y)]} \\
& \exp \left[-\frac{1}{T_c} (E_K \cosh y - K_L \sinh y) \left(\frac{\tau}{\tau_h} \right)^{1/3} e^{\kappa(\tau - \tau_h)/(2R_T)} \right] \} + \\
& \frac{g_\pi \tau_f}{\pi} \int_0^{2\pi} d\phi \int_0^{R_T} r_T dr_T \int_{-\infty}^{+\infty} dy [E_K \cosh y - K_L \sinh y] \\
& e^{i\tau[\frac{K_T}{E_K} q_T \cos \alpha \cosh y + q_L (\frac{K_L}{E_K} \cosh y - \sinh y)] - i q_T R_T \cos(\alpha - \phi)} e^{-\frac{1}{T_f} (E_K \cosh y - K_L \sinh y)} . \quad (36)
\end{aligned}$$

The five terms composing the correlation function represent, respectively, the emission from the quark and gluon initial stage, their contribution during the mixed phase, the pion emission also from the surface in that phase, the emission during the pure pionic phase up to reaching the freeze-out temperature, T_f , and finally, the volumetric instantaneous decoupling once it was reached.

Similarly, we can write the spectrum, as

$$\begin{aligned}
G(k_i, k_i) & \propto \kappa R_T \int_{-\frac{\pi}{2}}^{\frac{\pi}{2}} d\phi \cos \phi \int_{-\infty}^{+\infty} dy [E_i \cosh y - k_{iL} \sinh y] \\
& \{ g_{qgp} \int_{\tau_0}^{\tau_c} \tau d\tau \exp[-\frac{1}{T_0} (E_i \cosh y - k_{iL} \sinh y) \left(\frac{\tau}{\tau_0} \right)^{1/3} e^{\kappa(\tau - \tau_0)/(2R_T)}] + \\
& g_{qgp} \int_{\tau_c}^{\tau_h} \tau d\tau (f) e^{-\frac{1}{T_c} (E_i \cosh y - k_{iL} \sinh y)} + g_\pi \int_{\tau_c}^{\tau_h} \tau d\tau (1 - f) e^{-\frac{1}{T_c} (E_i \cosh y - k_{iL} \sinh y)} + \\
& g_\pi \int_{\tau_h}^{\tau_f} \tau d\tau \exp[-\frac{1}{T_c} (E_i \cosh y - k_{iL} \sinh y) \left(\frac{\tau}{\tau_h} \right)^{1/3} e^{\kappa(\tau - \tau_h)/(2R_T)}] \} + \\
& \frac{g_\pi \tau_f}{\pi} \int_0^{2\pi} d\phi \int_0^{R_T} r_T dr_T \int_{-\infty}^{+\infty} dy [E_i \cosh y - k_{iL} \sinh y] e^{-\frac{1}{T_f} (E_i \cosh y - k_{iL} \sinh y)} . \quad (37)
\end{aligned}$$

We remind that $G(k_i, k_i)$ is the spectrum as written in Eq.(3). If we then integrate separately the terms of Eq. (37) in $d^3 k_i/E_i$, i.e., in the intervals $\tau_0 \leq \tau \leq \tau_c$, $\tau_c \leq \tau \leq \tau_h$, $\tau_h \leq \tau \leq \tau_f$, and at $\tau = \tau_f$, we recover the number of emitted particles in each interval, as seen in Eq.(30), (31), (32), and (34), respectively, except for an overall normalization constant, which is cancelled when we estimate the interferometric relations, as in Eq. (1).

For estimating the (real) amplitudes $G(k_i, k_i)$ in the denominator of Eq. (1), we wrote $\mathbf{k}_1 = \mathbf{K} + \mathbf{q}/2$ and $\mathbf{k}_2 = \mathbf{K} - \mathbf{q}/2$, from the definition of the momenta \mathbf{K} and the relative momentum \mathbf{q} , since we are not generating the individual momenta and later averaging over all of them, as done in the experiment. In this first approach, that is the way we connected the momenta k_i in the spectra $C(k_i, k_i)$ to the momenta appearing in the complex amplitude, $C(k_1, k_2) = C(q, K)$.

This means that we can write

$$|\mathbf{k}_{T1,2}| = \sqrt{(\mathbf{K}_T \pm \mathbf{q}_T/2)^2} = \sqrt{\mathbf{K}_T^2 + \frac{\mathbf{q}_T^2}{4} \pm K_T q_T \cos \alpha} . \quad (38)$$

$$|k_{L1,2}| = \sqrt{K_L^2 + \frac{q_L^2}{4} \pm K_L q_L} ; E_{1,2} = \sqrt{m^2 + (\mathbf{K}_T \pm \mathbf{q}_T/2)^2 + (K_L \pm q_L/2)^2} . \quad (39)$$

In these equations, α is the angle between \mathbf{K}_T and \mathbf{q}_T .

Due to the azimuthal symmetry of the problem, we can choose \mathbf{K}_T along the x -axis, without any loss of generality. In this way, we see that the component of the relative momentum in the *outward* direction ($\mathbf{q}_T \parallel \mathbf{K}_T$), $\mathbf{q}_{T_{out}}$, will be along the x -axis, while the *sideward* component ($\mathbf{q}_T \perp \mathbf{K}_T$), $\mathbf{q}_{T_{sid}}$, will be directed along the y -axis, i.e., $q_x = q_{T_{out}}$ and $q_y = q_{T_{sid}}$. This implies that, in the first case, we chose $\alpha = 0$ and, in the second, $\alpha = \pi/2$.

In order to check how the spectra estimated within our model and the above discussed relations behave compared to data (PHENIX minimum bias [13]), we plot the single-inclusive distribution in Fig. 3. From here on we limit our estimates and discussions to the central rapidity region, i.e., $y_i = 0$ (which implies that $k_{i_L} = 0$, and, consequently, $K_L = 0$ and $q_L = 0$). In Fig. 3, we show the spectra, within a constant arbitrary normalization for the set of interrelated values shown in the first line of Table 1, and for two values of the emissivity, $\kappa = 0.5, 1$. We see that both curves describe well the spectrum in the low momentum region of the pions, up to roughly $k_{iT} \approx 1$ GeV/c. We shall consider these possibilities also when studying the correlation function and fitted radii.

In Fig. 4 we show the correlation functions $C(q_{T_{out}})$ vs. $q_{T_{out}}$ (solid curves), corresponding to $\alpha = 0$, and $C(q_{T_{sid}})$ vs. $q_{T_{sid}}$ (dashed ones, very close to one another), for $\alpha = \pi/2$, in the same plot for better visualize the differences. When calculating the correlation function in terms of $q_{T_{out}}$, we fixed $q_{T_{sid}} = 0$ (remember that we had already fixed $q_L = 0$, as a simplifying assumption). They are displayed for three values of the average pair momentum, $K_T = 0.17, 0.47$, and 0.80 GeV/c, and emissivity $\kappa = 1$.

In Fig. 5, we illustrate the behavior of the correlation functions, $C(q_{T_{out}})$ vs. $q_{T_{out}}$ (solid curves) and $C(q_{T_{sid}})$ vs. $q_{T_{sid}}$ (dashed curves), similarly to Fig.4, but with emissivity $\kappa = 0.5$. Again, the curves were estimated for $K_T = 0.17, 0.47$, and 0.80 GeV/c. We see that in this case the correlation functions versus $q_{T_{out}}$ are always narrower (consequently, the radii are bigger) than those curves versus $q_{T_{sid}}$. This originates in the higher contribution from the volumetric term with respect to the surface ones, coming from their lower emissivity in this case, since $\kappa = 0.5$ in that plot. The larger emission duration is also a consequence of this reduced surface emissivity with respect to the previous case discussed in Fig. 4.

Although not shown for sake of clarity in the plots, the correlation functions, $C(q_{T_{out}}) \times q_{T_{out}}$ and $C(q_{T_{sid}}) \times q_{T_{sid}}$, were also computed for other three values of K_T , i.e., all together, for $K_T = 0.17, 0.27, 0.38, 0.47, 0.63$, and 0.80 GeV/c. Each of the curves, either for $\kappa = 0.5$ or for $\kappa = 1$, were fitted by Gaussian distributions, in the regions where their behavior could be reasonably well approximated to that distribution. In this way, we obtained the corresponding average values of R_{out} and R_{sid} , as shown in Fig. 6 and 7, and from those, we estimated the ratio R_{out}/R_{sid} . We see that R_{sid} as a function of K_T is basically flat in both cases, since we have considered no transverse flow in the computations. However, our R_{out} decreases with increasing K_T , although not as much as suggested by data. This is a consequence of the time dependence of the temperature, that the higher momentum particles are emitted at earlier times. The values obtained for the ratio are plotted in Fig. 8 together with the preliminary STAR (filled triangles) and PHENIX (filled circles) data for both π^+ and π^- . We can see that our results were highly successful in describing both sets of data for $\kappa = 1$, but the curve corresponding to $\kappa = 0.5$ is away above the data limits, suggesting that we should have a high emissivity along the system history in order to explain the data trend.

VI. SUMMARY AND CONCLUSIONS

This simple model works well for the ratio of R_{out}/R_{sid} and suggests that the origin of the experimental value lies in the opacity of source emission and the relatively short time of decoupling of the longitudinal expansion, i.e., of the order of the nuclear radius. The principal reason why we are able to get such a small ratio of R_{out}/R_{side} is probably due to a combination of two effects. The first is that the surface is opaque, and whatever is emitted from the surface will have a small value of this radius. The second effect is that we allow black body radiation by gluons when the surface is very hot. This allows a much larger contribution from surface emission than is typical of what happens in hydrodynamical simulations where particles are emitted by Cooper-Frye decoupling from a surface at very low temperature. In fact we find that about 80% of the emission comes from the surface. The fact that so many particles are emitted from the surface at early times also means that the longitudinal decoupling time in this computation is significantly shorter than would be the case for hydrodynamic simulations, and this again goes in the direction suggested by the RHIC data, where the longitudinal time scale did not grow as much as might have been expected between SPS and RHIC energies.

The model also describes the typical source radii reasonably well, but not the K_T dependence of these radii, as seen in Figs. 6 and 7. This suggests that the time variation of the emitting radius and the introduction of transverse flow may play a significant role, [16]- [18]. If there is a time variation of the various radii, this will be correlated with the typical momentum scale of emitted particles, since the earlier is the time, the hotter are the particles. We are sensitive to such variation since we allow emission from the hot surface at early time. Also, a proper treatment of the decoupling is not included in our computations and this certainly will affect the results, although it might also suggest modification in the treatment of decoupling, [18], [19].

At a minimum, these computations suggest that the problem in describing the various HBT ratios lies not so much in R_{out}/R_{sid} as it does in computing the full set of radii and obtaining a comprehensive and complete description of all of the above within one dynamical model. The ratio of R_{out}/R_{sid} may very well be independent of many of the variations within these models since it is dimensionless, where the dimensionful values of the various radii are sensitive to changes of time and size scales. Such a complete dynamical computation allowing the possibility of surface emission at very early times has not been implemented. It may in fact be more complicated than we suggest: Perhaps the surface emissivity is a strong function of the momentum of the emitted particles. We certainly expect that high momentum particles are more easily emitted than are low momentum ones.

ACKNOWLEDGMENTS

S.S.P. would like to express her gratitude to the Nuclear Theory Group at BNL for their kind hospitality and for the stimulating discussion atmosphere during the elaboration of this work. She would also like to thank R. Keith Ellis and the Theoretical Physics Dept. at Fermilab, for their kind hospitality. Both of the authors would like to thank Ulrich Heinz and Peter Kolb for discussions on an earlier version of this manuscript, and the referees of the paper for their meticulous reading and suggestions, pointing out an error in the estimate of the multiplicity. This research was partially supported by CNPq under Proc. N. 200410/82-2. This manuscript has been authored under Contracts No. DE-AC02-98CH10886 and No. DE-AC02-76CH0300 with the U.S. Department of Energy.

REFERENCES

- [1] F. Laue, Proc. Quark Matter 2001, Nucl. Phys. A698 (2002) 177c; C. Alder et al., STAR Collab., Phys. Rev. Lett. 87 (2001) 082301.
- [2] S. Johnson: "RHIC, PHENIX, HBT and other acronyms", RHIC/INT Winter Workshop 2002 on "Correlations and Fluctuations in Heavy-Ion Collisions at RHIC", Seattle, Jan 4-6 2002; K. Adcox et al, Phys. Rev. Lett. 88 (2002) 192302.
- [3] H. Heiselberg and A. P. Vischer, Eur. Phys. J. C1 (1998) 593; H. Heiselberg, Phys. Lett. B421 (1998) 18.
- [4] B. Tomášik and U. Heinz, nucl-th/9805016; Acta Phys. Slov. 49 (1999) 251.
- [5] For reviews on HBT for heavy ion collisions, see Refs. [6] and [14] below, as well as: W.A. Zajc, Hadronic Multiparticle Production, World Scientific Press, P. Carruthers, ed. (1988); D.H. Boal, C.K. Gelbke and B.K. Jennings, Rev. Mod. Phys. 62 (1990) 553; C-Y. Wong, *Introduction to High-Energy Heavy-Ion Collisions*, World Scientific (1994); R.M. Weiner, *Bose-Einstein Correlations in Particle and Nuclear Physics*, J. Wiley & Sons (1997); T. Csörgő, Heavy Ion Phys. 15 (2002) 1-80.
- [6] U. Heinz and B. Jacak, Ann. Rev. Nucl. Part. Sci. 49 (1999) 529.
- [7] S. Pratt, Phys. Rev. D33 (1986) 1314 ; Y. Hama and Sandra S. Padula, Phys. Rev. D37 (1988) 3237; G. F. Bertsch, Nucl. Phys. A498 (1989) 173c.
- [8] U. Heinz and P. Kolb, Nucl. Phys. A702, 269 (2002).
- [9] B. Tomášik, U. A. Wiedemann, and U. Heinz, nucle-th/9907096.
- [10] H. Appelshäuser et al., NA49 Collaboration, Eur. Phys. J. C2 (1099) 661.
- [11] R. A. Soltz, M. Baker, and J. H. Lee, Nucl. Phys. A661 (1999) 439c.
- [12] J. D. Bjorken, Phys. Rev. D27 (1983) 140.
- [13] K. Adcox et al., Submitted to PRL, preprint nucl-ex/0112006.
- [14] M. Gyulassy, S.K. Kaufmann, and L.W. Wilson, Phys. Rev. C20 (1979) 2267; K. Kolehmainen and M. Gyulassy, Phys. Lett. B180 (1986) 203.
- [15] M. Gyulassy and Sandra S. Padula, Phys. Lett. B217 (1989) 181; Sandra S. Padula, M. Gyulassy, and S. Gavin, Nucl. Phys. B329 (1990) 357 ; Sandra S. Padula and M. Gyulassy, Nucl. Phys. B339 (1990) 378.
- [16] U. Heinz and P. Kolb, hep-ph/0204061.
- [17] Tetsufumi Hirano, Keiichi Tsuda, and Kohei Kajimoto, nucl-th/0011087.
- [18] D. Teaney, J. Lauret, and Edward V. Shuryak, Phys. Rev. Lett. 86 (2001) 4783.
- [19] S. Soff, S. A. Bass, and A. Dumitru, Phys. Rev. Lett. 86 (2001) 3981.

FIGURES

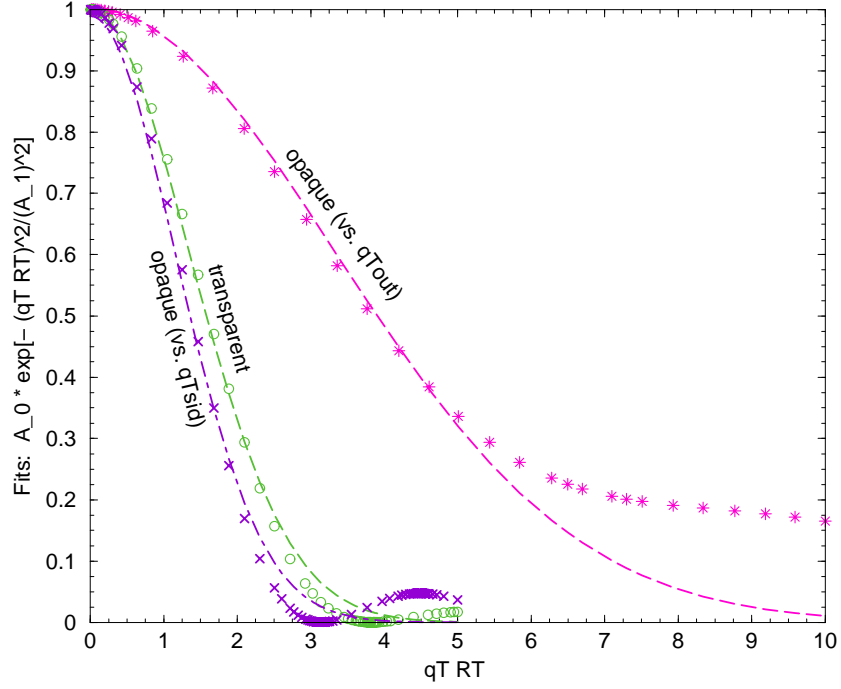


FIG. 1. Illustration of the correlation functions in the *very simple model* for R_{out} and R_{sid} as a function of the corresponding variable qT_{out} and qT_{sid} . For emphasizing the geometrical differences, we considered $\Delta t = 0$ in the plots of the $C(qT_{out})$ vs. qT_{out} . The set of points and the fitting curve in the middle correspond to both $C(qT_{out})$ vs. qT_{out} and $C(qT_{sid})$ vs. qT_{sid} in the transparent case, since **no** time dependence is included in the qT_{out} variable in the above plot. The narrower and the wider sets correspond, respectively, to $C(qT_{sid})$ vs. qT_{sid} and to $C(qT_{out})$ vs. qT_{out} in the opaque case. We see that, as a result of the opacity of the source, this last set is much broader than the first one.

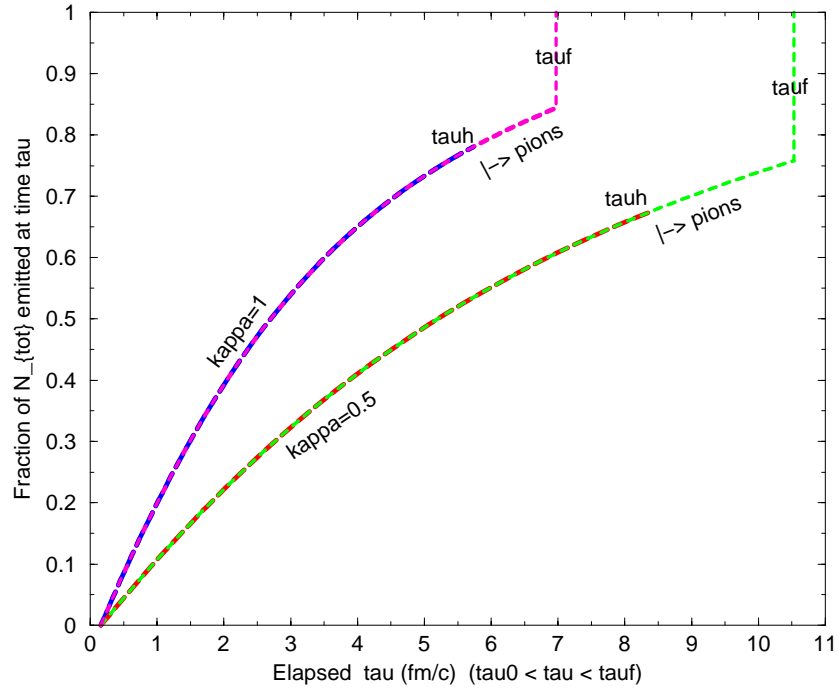


FIG. 2. The flux of emitted particles per unit time is shown, normalized to their total number, for two values of the emissivity ($\kappa = 1$ and $\kappa = 0.5$), at each instant, starting at $\tau_0 = 0.16$ fm/c, passing by the beginning of the phase transition, at $\tau = \tau_c$, then through its end at τ_h , and finally, stopping at the instant when the pionic system reaches τ_f . We clearly see the fraction of the pions still in the system at that instant, which is then immediately emitted from the entire volume. In this example, we fixed $T_0 = 411$ MeV, $T_c = 175$ MeV, $T_f = 150$ MeV, $R_T \approx 7$ fm/c, and the number of quark flavors in the QGP phase to be 2.

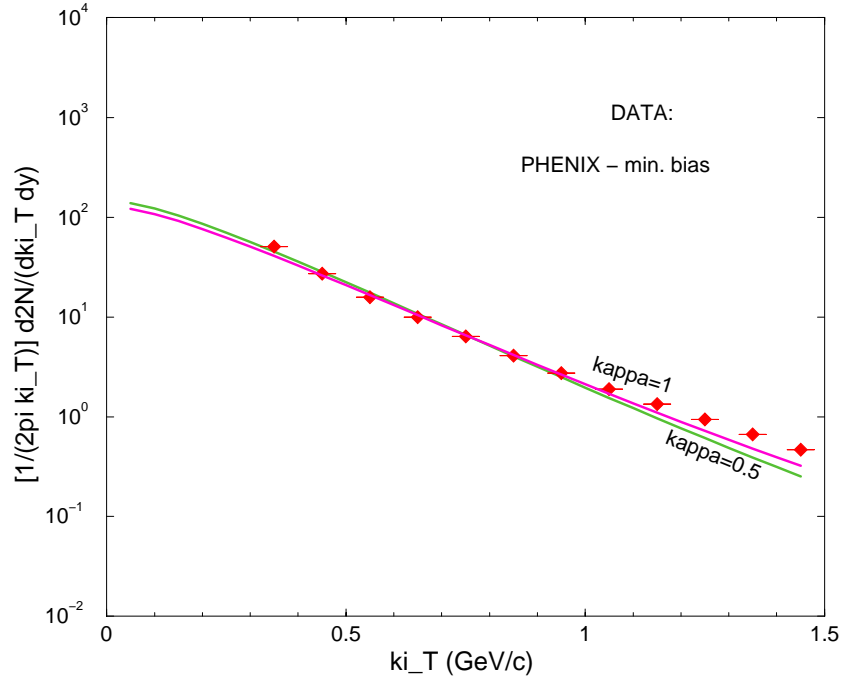


FIG. 3. The prediction based on our model for the transverse momentum distribution of emitted pions is shown. The points are from the minimum-bias data from PHENIX Collaboration. The curves correspond to emissivity $\kappa = 0.5$ and to $\kappa = 1$, without the inclusion of transverse flow. We see that both cases describes data on spectrum well in the low pion momentum region, up to about $k_{iT} \approx 1$ GeV/c. The parameters used are explained in the text, corresponding to $T_0 = 411$ MeV, $T_c = 175$ MeV, $T_f = 150$ MeV, and the transverse radius, $R_T \approx 7$ fm/c.

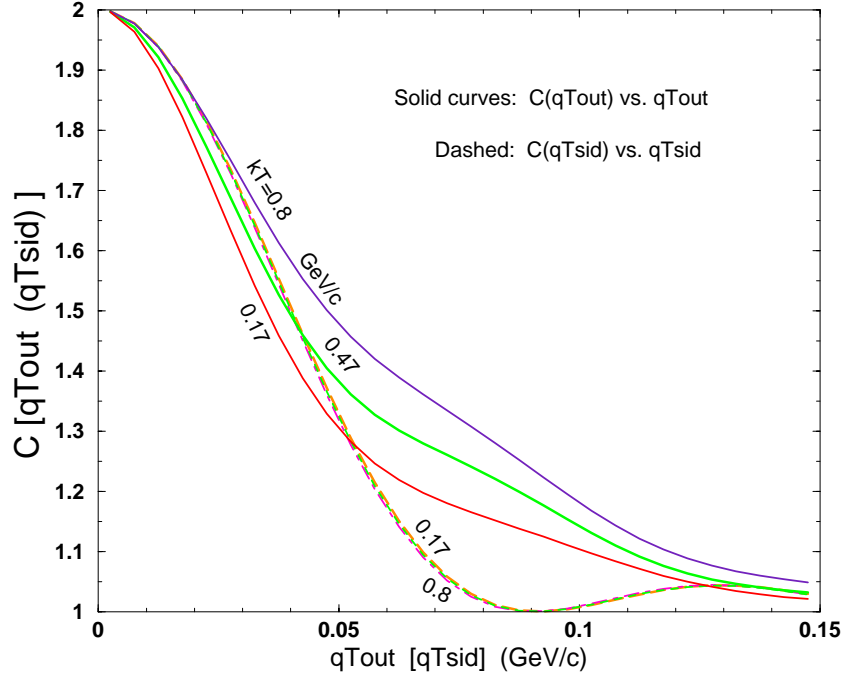


FIG. 4. The correlation functions, $C(q_{T_{out}}, K_T)$ vs. $q_{T_{out}}$ (solid), and $C(q_{T_{sid}}, K_T)$ vs. $q_{T_{sid}}$ (dashed), are shown for three distinct values of the average pair momentum, K_T , corresponding to the phase transition temperature $T_c = 175$ MeV, $T_f = 150$ MeV, including a volumetric emission when the hadronic (pions) system reaches $\tau = \tau_f$. We see that the width of the curves as function of $q_{T_{out}}$ increase (or conversely, the radii decrease) with increasing K_T , whereas the curves for different $q_{T_{sid}}$ show no visible variation, as would be expected since no transverse flow is considered in the computation. The same input parameters were adopted here: $T_0 = 411$ MeV, $T_c = 175$ MeV, $T_f = 150$ MeV, the transverse radius, $R_T \approx 7$ fm/c, and emissivity $\kappa = 1$.

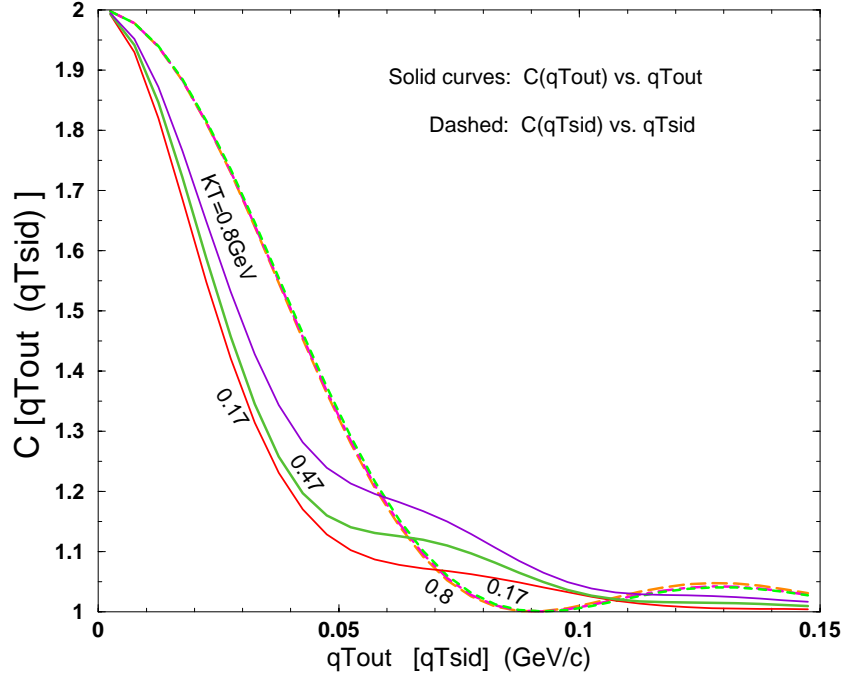


FIG. 5. The correlation functions, $C(q_{T_{out}}, K_T)$ vs. $q_{T_{out}}$ (solid), and $C(q_{T_{sid}}, K_T)$ vs. $q_{T_{sid}}$ (dashed), are shown for three distinct values of the average pair momentum, K_T , as in Fig. 4, but now with reduced emissivity, $\kappa = 0.5$. We see that the width of the solid curves still increase (or conversely, the radii decrease) with increasing K_T , but they are all smaller than the width corresponding to the dashed curves. The same input parameters as before were adopted here: $T_0 = 411$ MeV, $T_c = 175$ MeV, $T_f = 150$ MeV, the transverse radius, $R_T \approx 7$ fm/c.

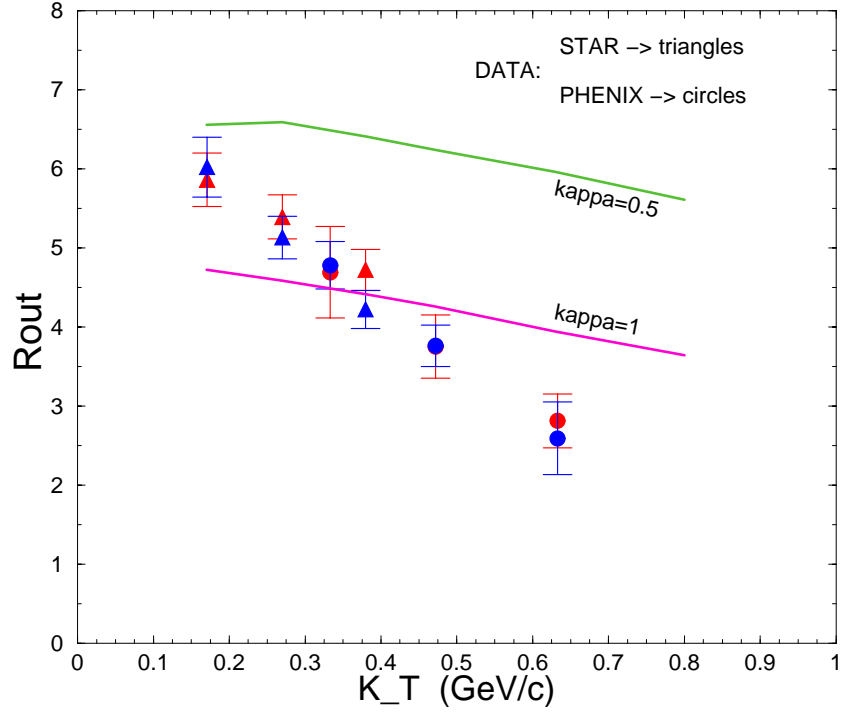


FIG. 6. Our results for R_{out} (*outward*) radius are shown as a function of the average pair momentum, K_T , for the two cases discussed before, corresponding to 50% emissivity and to $\kappa = 1$, without inclusion of transverse flow. The experimental data points from STAR (triangles) and PHENIX (circles) are also included in the plot. The values of the parameters are the same as in the previous plots, i.e., $T_0 = 411$ MeV, $T_c = 175$ MeV, $T_f = 150$ MeV, the transverse radius, $R_T \approx 7$ fm/c.

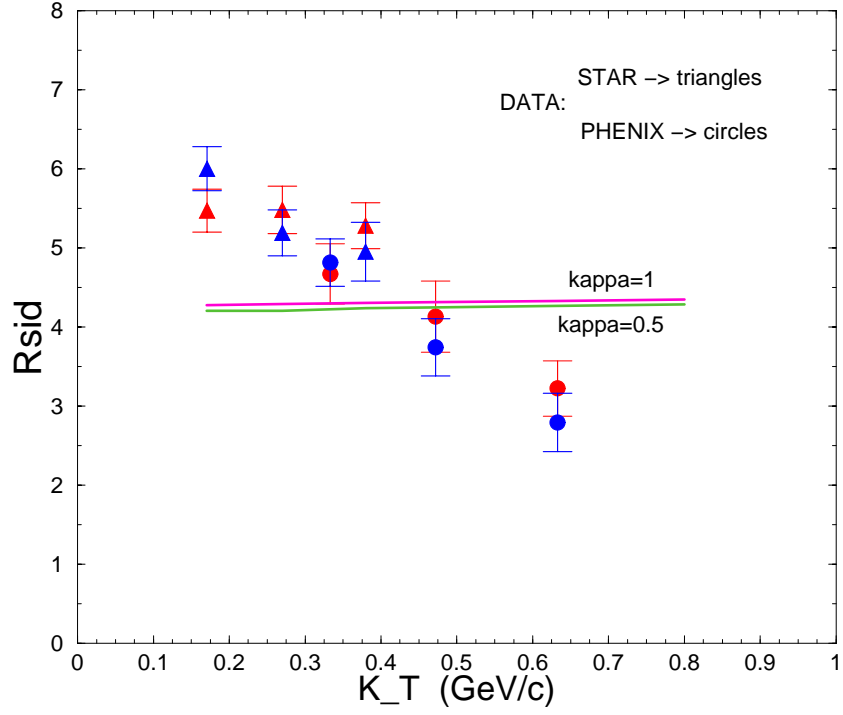


FIG. 7. Analogously to the previous case, we show here the results for R_{sid} (*sideward*) radius vs. K_T , studied for $\kappa = 0.5, 1$. No sensitivity to κ is seen, since no transverse flow is included in the computation. The experimental data points with error bars are from STAR (triangles) and PHENIX (circles). The values of the parameters are the same as in the previous plots, i.e., $T_0 = 411$ MeV, $T_c = 175$ MeV, $T_f = 150$ MeV, and the transverse radius, $R_T \approx 7$ fm/c.

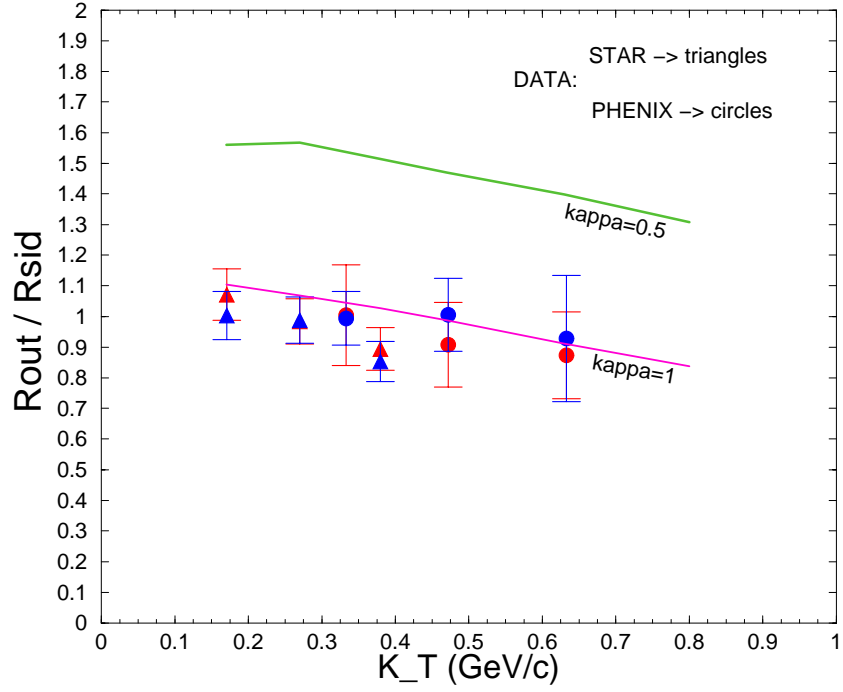


FIG. 8. The result corresponding to the ratio R_{out}/R_{sid} of the *outward* radius by the *sideward* one is shown within our model. We see that the ratio corresponding to full emissivity ($\kappa = 1$) agrees very well with data within the experimental error bars (shown in the plot), whereas the 50% emissivity case is completely excluded by data, since the ratio is too high in that case, reflecting what we saw in the two previous plots. The values of the parameters are the same as before, i.e., $T_0 = 411$ MeV, $T_c = 175$ MeV, $T_f = 150$ MeV, and the transverse radius, $R_T \approx 7$ fm/c.